Structural characterization and physicochemical properties of exopolysaccharide from moderate halophile Chromohalobacter salexigens, strain 3EQS1

Ibrahim M. Ibrahim
Fayoum University
Yuliya P. Fedonenko (fedonenko_yu@ibppm.ru)
Institute of Biochemistry and Physiology of Plants and Microorganisms
Elena N. Sigida
Institute of Biochemistry and Physiology of Plants and Microorganisms
Maxim S. Kokoulin
Pacific Institute of Bioorganic Chemistry. GB Elyakova Far Eastern Branch of the Russian Academy of Sciences
Vyacheslav S. Grinev
Institute of Biochemistry and Physiology of Plants and Microorganisms
Ivan G. Mokrushin
Perm State University
Gennady L. Burygin
Institute of Biochemistry and Physiology of Plants and Microorganisms
Andrey M. Zakharevich
Saratov State University
Alexander A. Shirokov
Institute of Biochemistry and Physiology of Plants and Microorganisms
Svetlana A. Konnova
Saratov State University

Research Article

Keywords: Chromohalobacter salexigens, Extracellular polysaccharide, Levan, Emulsifying activity, Biosurfactant

Posted Date: June 16th, 2022

DOI: https://doi.org/10.21203/rs.3.rs-1742495/v1

Abstract

A strain, 3EQS1, was isolated from a salt sample taken from Lake Qarun (Fayoum Province, Egypt). On the basis of physiological, biochemical, and phylogenetic analyses, the strain was classified as *Chromohalobacter salexigens.* By 72 h of growth at 25 °C, strain 3EQS1 produced large amounts (15.1 g L^{-1}) of exopolysaccharide (EPS) in a liquid mineral medium (initial pH 8.0) containing 10% sucrose and 10% NaCl. The EPS was precipitated from the cell-free culture medium with chilled ethanol and was purified by gel-permeation and anion-exchange chromatography. The molecular mass of the EPS was 0.9×10^6 Da. Chemical analyses, Fourier transform infrared spectroscopy, and nuclear magnetic resonance spectroscopy showed that the EPS was a linear β-d-(2→6)-linked fructan (levan). In aqueous solution, the EPS tended to form supramolecular aggregates with a critical aggregation concentration of 240 μg mL^{-1}. The EPS had high emulsifying activity (E_{24}, %) against kerosene (31.2 ± 0.4%), sunflower oil (76.9 ± 1.3%), and crude oil (98.9 ± 0.8%), and it also had surfactant properties. A 0.1% (w/v) aqueous EPS solution reduced the surface tension of water by 11.9%. The levan of *C. salexigens* 3EQS1 may be useful in various biotechnological processes.

Introduction

Saline and hypersaline environments form the largest ecosystem on the earth, containing a rich variety of organisms from all three domains of life (Oren 2015). In addition, much of the earth's freshwater and land is exposed to salinization and, therefore, is limited in use or may be unsuitable for human activity (Ondrasek and Rengel 2021). Advances in industrial technology have increased environmental pollution by organic compounds (mostly crude oil and petroleum products), and not surprisingly, halophilic microorganisms, which survive under extreme conditions, have become the most promising agents for bioremediation and biotechnological use (Oren 2010; Zhuang et al. 2010; Ławniczak et al. 2020). The use of halophilic and halotolerant microbes in the biodegradation of organic pollutants has been repeatedly reviewed (Le Borgne et al. 2008; Sorokin et al. 2012; Fathepure 2014; Edbeib et al. 2016).

The halophilic γ-proteobacteria that degrade aliphatic and aromatic hydrocarbons in hypersaline environments include Halomonadaceae members (Khalil et al. 2021). Of the 16 Halomonadaceae genera (Ventosa et al. 1998; Arahal et al. 2007), those including the largest number of halophilic and halotolerant species are *Cobetia* (5 species), *Chromohalobacter* (9 species), *Deleya* (8 species), *Halomonas* (106 species), *Kushneria* (9 species), and *Salinicola* (12 species). Halophilic members of the Halomonadaceae are promising sources of compatible solutes (powerful stabilizers of biomolecules and cells), salt-tolerant enzymes, biosurfactants, and extracellular polysaccharides (EPSs) (Oren 2010; Argandoña et al. 2012; Corral et al. 2020).

Bacteria of the family Halomonadaceae synthesize a variety of extracellular polymeric substances, including polysaccharides, which form the surrounding layer of cells and are intensely secreted by the cells into their environment (de la Haba et al. 2011). Halophilic eubacteria (γ-Proteobacteria and Firmicutes) produce fructans (often of the levan type), which are engaged in biotic stress resistance

mechanisms and in signaling processes (Kirtel et al. 2018). Fructans are some of the most abundant functional biomolecules in nature and are an important class of platform chemicals. The production of fructans by microbial systems is preferable, because this bioprocess can be optimized and controlled.

Levan-producing halophiles are of particular interest, because they elaborate the polysaccharide in nonsterile (highly saline) environments, even in seawater (Kazak Sarilmişer et al. 2015; Toksoy Öner et al. 2016), and are possible genetic sources of industrial compounds such as osmolytes, biosurfactants, and extremozymes (Chen and Jiang 2018). Recently, levan-producing bacteria have been isolated from oil-polluted sources (Kekez et al. 2015; Djurić et al. 2017; Mendonça et al. 2021). Husseiny et al. (2015) showed the potential of a *Chromohalobacter salexigens* strain to produce levan and determined the antitumor, fibrinolytic, and prebiotic activities of the levan and its sulphated and carboxymethylated derivatives. Here we characterize *Chromohalobacter salexigens* strain 3EQS1, isolated from a salt sample from Lake Qarun (Fayoum Province, Egypt), and we report the structure and properties of its extracellular high-molecular-mass levan.

Materials And Methods

Isolation and identification of *Chromohalobacter salexigens* 3EQS1

Originally, different halophilic strains were isolated fromuntreated salt samples collected in June 2020 from Lake Qarun (Fayoum Province, Egypt; 29° 27' 13" N, 30° 34' 51" E, 45 m below sea level) by standard serial dilution and plating techniques (Ibrahim et al. 2020). The isolates were subcultured on agar plates containing a standard growth medium of the following composition (g L^{-1}): casamino acids, 7.5; glucose, 10; sucrose, 10; yeast extract, 10; $MgSO_4 \times 7H_2O$, 20; KCl, 2; $Na_3C_6H_5O_7 \times 2H_2O$, 3; agar, 20 (pH 7.5) (Sehgal and Gibbons 1960). NaCl was added at 0 to 25% (w/v), and the plates and incubated at 25 °C for 48–72 h. Morphologically distinct EPS-producing mucoid colonies were selected for further validation. Five isolates with a mucoid phenotype grew in a wide NaCl concentration range. Of these isolates, strain 3EQS1 was chosen as the most prolific EPS producer.

Strain 3EQS1 was subjected to morphological and biochemical characterization, as described in Ibrahim et al. (2020), and to molecular identification. Some enzymatic activities were tested with the API-20E and 50CH systems (bioMérieux, Lyon, France) by using 10% (w/v) NaCl. The assignment of the strain to the *Chromohalobacter* species was confirmed with a Biolog GP Microplate miniaturized biochemical system (Biolog, Hayward, CA, USA). Genomic DNA was extracted from 1 mL of a bacterial suspension (2×10^7 cells mL^{-1}) with a QIAamp DNA mini kit (Qiagen, Germany), as recommended by the manufacturer. The 16S rDNA was amplified with two universal primers, 27F (5' AGAGTTTGATCCTGGCTCAG 3') and 1492R (5' AAGGAGGTGATCCAGCCGCA 3'). The amplified DNA products were separated on agarose gels and were recovered with a NucleoTrap gel extraction kit (Macherey-Nagel, Duren, Germany). The nucleotide sequence of the purified bands was determined with an ABI PRISM 3500xL genetic analyzer (Applied Biosystems, USA). The isolate was identified through the BLASTn online program (National Center for Biotechnology Information, http://www.ncbi.nlm.nih.gov/gquery/?term=blastn) and also

through the EzTaxon-e server (http://www.ezbiocloud.net/), on the basis of 16S rRNA gene sequence data (Kim et al. 2012). A phylogenetic tree was constructed by the neighbor-joining method with FastME (Lefort et al. 2015). Confidence in the branching points was established by bootstrap analysis (1000 replicates). The 16S rRNA gene sequence of strain 3EQS1 was deposited in the GenBank under accession number OK189068.

Isolation and purification of EPS

Strain 3EQS1 was grown in a modified liquid nutrient broth composed as follows (g L^{-1}): sucrose, 20 (or glucose, 20, or lactose, 20, or fructose, 20, or mannose, 20); yeast extract, 4; $MgSO_4 \times 7H_2O$, 20; KCl, 2; $Na_3C_6H_5O_7 \times 2H_2O$, 3; NaCl, 0, 50, 100, 150, and 250. Growth was conducted at 25 °C for 72 h in 1 L Erlenmeyer flasks, each containing 350 mL of the medium, in an ES-20/60 orbital shaker–incubator (Biosan, Latvia; 180 rpm). The initial pH of the medium was 8.0. The effect of the sucrose concentration (30, 50, 100, and 150 g L^{-1}) was evaluated at 10% (w/v) NaCl. Before inoculation, a filtered carbohydrate solution (polytetrafluoroethylene filter; pore size, 0.46 μm; Pall Corporation, USA) was added to the medium. The culture broth was centrifuged at 4000 ´ *g* for 30 min to separate cells from the supernatant liquid. The cell-free supernatant liquid was evaporated to a minimal volume at 40 °C under reduced pressure (Laborota 4000; Heidolph, Germany). Salts and low-molecular-mass compounds were removed by dialysis against distilled water at 4 °C for 48 h (molecular mass cut-off of the cellulose membrane, 13 kDa; Sigma-Aldrich Chemie, Seelze, Germany). The dialyzed supernatant liquid was concentrated, and the crude EPS was precipitated by slowly pouring a threefold volume of chilled ethanol into the supernatant liquid and stirring the mixture at 200 rpm with an overhead stirrer (Microstar 7.5 control; IKA, Germany). The precipitate was separated by centrifugation at 3000 ´ *g* for 20 min, washed repeatedly with chilled ethanol, resuspended in water, and lyophilized in a Benchtop 2K freeze dryer (VirTis, USA).

The crude EPS was fractionated by gel-permeation chromatography (GPC) (Sepharose CL-6B column, 2.5×50 cm; GE Healthcare, USA), with 0.025 M NH_4HCO_3 as the eluent (flow rate, 30 mL h^{-1}). The EPS-containing fractions were pooled and lyophilized for further purification by anion-exchange chromatography (DEAE Toyoperl 650M column, 1.5×40 cm; Supelco, Germany). The buffer was Tris-HCl (pH 7.2), the NaCl gradient was from 0 to 1 M, and the flow rate was 60 mL h^{-1}. The purified EPS was lyophilized, and its structure was characterized.

General analytical techniques

Total carbohydrates and proteins were measured by the methods of DuBois et al. (1956) and Bradford (1976), respectively. The instrument used was a Specord 40 spectrophotometer (Analytik Jena AG, Germany).

The monosaccharide composition of the EPS (2 mg) was analyzed after hydrolysis in 0.01 M H_2SO_4 at 80 °C for 2 h, followed by neutralization with 5 M NaOH. The analysis was done by high-performance

anion-exchange chromatography with pulsed amperometric detection (HPAEC–PAD), by using a Smartline 5000 instrument (Knauer, Germany) equipped with a CarboPac PA-20 column.

The average molecular mass of the EPS was determined by high-performance gel-permeation chromatography (HPGPC; Smartline 5000, Knauer), by using a 7.8 mm × 300-mm PolySep-GFC-P 5000 column (Phenomenex, Torrance, CA, USA; column temperature, 30 °C) and a refractive index detector. The concentration of the polysaccharide samples used for analysis was 1 mg ml^{-1}, the mobile phase was 0.2 M $NaNO_3$, and the flow rate was 0.5 mL min^{-1}. The system had been calibrated with dextrans as standards (20, 40, 70, 110, 229, 500, and 2000 kDa; Fluka, Germany). The molecular mass of the EPS was calculated from a standard curve.

Fourier transform infrared (FTIR) spectroscopy

Functional groups of the EPS were examined on a Nicolet 6700 FTIR spectrometer (Thermo Scientific, USA). The spectrum of dry air was used as the reference. The lyophilized EPS (2 mg) was ground with dried KBr powder (0.5 g) and pressed into a tablet under vacuum. The FTIR spectrum was recorded with an air dryer and with an H_2O and CO_2 absorber within the wave range 4000–400 cm^{-1} at a spectral resolution of 4 cm^{-1}. In total, not less than 64 scans were collected.

Nuclear magnetic resonance (NMR) spectroscopy

The EPS samples were deuterium exchanged by freeze-drying from D_2O. The ^{1}H and ^{13}C NMR spectra were recorded with an AVANCE DPX-500 instrument (Bruker Corporation, USA) at 313 K. 3-Trimethylsilylpropanoate-d_4 (δ_H 0.0 ppm) and acetone (δ_C 31.45 ppm) were used as internal standards. Two-dimensional (2D) experiments were done with standard Bruker software. TOCSY spectra were recorded at 200-ms duration of the MLEV-17 spin-lock, and ROESY spectra were recorded at 200-ms duration of the spin-lock. The HMBC spectrum was recorded with a 60-ms delay for the evolution of long-range spin couplings.

Thermogravimetric analysis allied with differential scanning calorimetry and mass spectroscopy (TGA-DSC-MS)

A levan sample was put in a platinum pan and was analyzed in an argon atmosphere on an STA 449 F1 Jupiter apparatus (Netzsch-Geratebau, Germany) equipped with a QMS 403 C Aëolos mass spectrometer (Netzsch-Geratebau). Heating was programmed to increase from 35 to 650 °C at 20 °C min^{-1}. The mass spectrometer was set to monitor the ions of common decomposition gases such as water (*m/z* 18), CO and/or N_2 (*m/z* 28), and CO_2 (*m/z* 44).

Scanning electron and atomic force microscopy

Scanning electron microscopy (SEM) of the EPS was done with a MIRA II LMU instrument (TESCAN, Czech Republic) operating at 4 kV in a secondary electron mode. Magnification ranged from 1000× to

20000×. Samples were prepared by air-drying a drop of an aqueous EPS solution (0.5%, w/v) on a silicon wafer at room temperature.

The topography of the dried samples was measured by atomic force microscopy (AFM) on an NTEGRA Spectra device (NTMDT, Russia) operating in a tapping mode and equipped with NSG10 tips (TipsNano, Russia). Samples were prepared by placing a 5-μL droplet of material on a glass substrate and drying it for several hours. All data (background subtraction, filtering of the feedback autogeneration frequency) were processed with Gwyddion software (Nečas and Klapetek 2012).

Dynamic light scattering (DLS) measurements

DLS analysis of the critical aggregation concentration (CAC) of aqueous EPS suspensions was done with a Malvern Zetasizer Nano ZS system equipped with a He-Ne laser (633 nm, 4 Mw; Malvern Instruments, UK). DLS was measured for concentrations ranging from 15.6 to 1 mg mL^{-1}. Measurements were made at 25 °C in a 10-mm polystyrene cell (Sarstedt, Germany) at a detection angle of 173° and at a constant aperture (attenuator 9). The measured scattering light intensity was displayed as a photon count rate with a unit of kilo counts per second (kcps). From the data of light scattering and the correction function of the scattering intensity fluctuations in time, we estimated the average hydrodynamic diameter (d) and the most probable modal hydrodynamic diameter (d_m) of the supramolecular particles (Burygin et al. 2016). Data were analyzed with DTS software (Version 4.2; Malvern Instruments, UK). The CAC was found at the intersection point of the two slopes of the curve of light scattering intensity versus EPS concentration (Aurell and Wistrom 1998).

Surfactant and emulsifying activities

The surfactant activity of the levan solution was evaluated by the oil displacement test. Briefly, 10 mL of distilled water was poured into Petri dishes and 100 μL of crude oil was added to the surface of the water. Then, 5 μL of an aqueous 0.1% (w/v) levan solution was spotted in the center of the crude oil surface. The area of the clear zone on the oil surface was measured 30 s later by comparison with 5 μL of distilled water (negative control) and 5 μL of 0.1% Triton X-100 (positive control) (Rodrigues et al. 2006).

The standard assay for emulsifying activity was based on a modification of the method of Cooper and Goldenberg (1987). The tested compounds included sunflower oil, kerosene, and crude oil. Briefly, 3 mL of oil or of a hydrocarbon was added to 2 mL of an EPS solution in distilled water (1%, w/v) in a glass tube and was vortexed for 5 min. After 24/48 h, the emulsion index ($E_{24/48}$, %) was calculated as given below:

$$E_{24/48} = h_e / h_T \times 100,$$

where h_e is the height of the emulsion layer (mm) and h_T is the overall height of the mixture (mm). All samples were kept at 25 °C. All tests were done in triplicate.

Surface tension measurements

These were made by the Wilhelmy plate method with an EasyDyne K20 tensiometer (Krüss, Germany) equipped with a thermostated jacket. The measurements were made at 30 °C with two concentrations of aqueous polysaccharide solutions¾0.5% and 0.1% (w/v). Milli-Q quality water was used to calibrate the instrument. Before every single measurement, the platinum plate was cleaned with isopropyl alcohol, heated in a flame, and cooled to room temperature.

Statistics

All measurements were replicated at least three times. Data are expressed as mean ± standard deviation (SD). Statistical differences between samples were determined with the significance level at $p < 0.05$.

Results

Phenotypic characterization and phylogeny

Strain 3EQS1, isolated from salt samples collected from Lake Qarun (Fayoum, Egypt), was analyzed for its ability to produce EPS. On the solid standard growth medium with 5% NaCl, the strain formed circular, umbonate, cream-pigmented, opaque, smooth mucoid colonies an indication of high EPS production. Of note, the strain did not form opaque colonies on the same medium with 25% NaCl. The cells were gram-negative, non-endospore-forming, straight rods with rounded ends. The cells occurred singly and occasionally in pairs, and they were motile and aerobic. Their size was 0.7–0.9 · 2.0–2.4 µm. Table 1 summarizes the phenotypic characterization of strain 3EQS1. With sucrose as the substrate, the strain produced large amounts of EPS.

Table 1
Comparative analysis of phenotypic features of strain 3EQS1 and its nearest phylogenetically related *Chromohalobacter* species

Characteristics	Strains		
	3EQS1	*C. salexigens* ATCC 33174[a]	*C. israelensis* ATCC 43985[Tb]
Cell morphology	Straight rods with rounded ends	Rods	Straight rods with rounded ends
Cell size (μm)	0.7–1.0×1.8–3.0	0.7–1.0×2.0–3.0	0.6–0.9×1.5–4.2
Motility		+	nd
Pigmentation	Cream, opaque	Cream, opaque	Cream
NaCl range (optimum) (%, w/v)	0–25 (5)	0.9–25 (7.5–10)	3.5–20(8)
Temperature range (optimum) (°C)	10–40 (35)	15–45 (37)	15–45 (30)
pH range (optimum)	5–10 (8)	5–10 (7.5)	5–9 (Nd)
Indole production	-	-	+
Oxidase/catalase activities	-/+	-/+	-/+
H_2S production	+	+	-
Urease	+	+	-
Citrate utilization	+	+	-
Nitrate reduction	+	+	+
Anaerobic growth with nitrate	+	+	-
Acid production from			
l-Arabinose	+	+	+
Maltose	-	+	+
Sucrose	+	+	+
Trehalose	-	-	-
Hydrolysis of casein	+	+	-
Growth on			

+ Positive, - negative, nd no data; [a] Data from Arahal et al. (2001); [b] Data from Huval et al. (1995).

Characteristics	Strains		
	3EQS1	*C. salexigens* ATCC 33174[a]	*C. israelensis* ATCC 43985[Tb]
Cellobiose	-	-	+
Sucrose	+	+	+

+ Positive, - negative, nd no data; [a] Data from Arahal et al. (2001); [b] Data from Huval et al. (1995).

Phylogenetic analysis of 16S rDNA gene sequences showed that strain 3EQS1 clustered with the type strains *Chromohalobacter salexigens* ATCC33174^T (Arahal et al. 2001) and *C. israelensis* ATCC43985^T (Huval et al. 1995), with 100 and 99.69% identity, respectively (Fig. 1). However, the phenotypic differences from *C. israelensis* (Table 1) led us to unambiguously assign strain 3EQS1 to the species *C. salexigens*. *C. salexigens* strain 3EQS1 was deposited in the IBPPM RAS Collection of Rhizosphere Microorganisms (Saratov, Russia; http://collection.ibppm.ru/) under accession number IBPPM 676.

Factors affecting *C. salexigens* 3EQS1 growth and EPS production

Strain 3EQS1 utilized several mono- and disaccharides as carbon sources but produced the most EPS when grown with sucrose (Fig. 2a). The strain grew with 0 to 25% NaCl, but as noted above, growth was optimal with 5% NaCl. When the salt concentration in the nutrient medium was increased to 10-15%, the EPS yield per gram of cells increased (Fig. 2b). Subsequently, the effect of the sucrose concentration on the EPS yield was examined with 10% NaCl. A stepwise increase in the sucrose concentration led to an increase in the EPS yield. With 3% sucrose, the yield was 6.9 g L^{-1}; with 5% sucrose, it was 8.3 g L^{-1}; and with 10% sucrose, it was 15.1 g L^{-1}. Further increasing the sucrose concentration (up to 15%) even led to a decrease in the EPS yield (12 g L^{-1}). Because members of the Halomonadaceae produce levans and because strain 3EQS1 produced increased amounts of EPS when grown with increasing sucrose concentrations, we speculated that the EPS of strain 3EQS1 is a levan-type fructan.

TGA-DSC-MS

The thermal behavior of the EPS and the nature of its degradation products were determined by synchronous TGA and DSC with MS detection of the gases formed in the degradation. TGA of the levan first showed a weight loss of 4.40% when the temperature rose above 100 °C (Fig. 3). This was assigned to the loss of residual moisture, which was confirmed by the presence of only water (*m/z* 18), as detected by MS (Fig. S1). The EPS remained stable at up to about 210 °C and then began to decompose, as confirmed by a large and sharp endothermic peak in the DSC curve. The thermal decomposition was attended by release of CO_2 and H_2O, which were clearly detected by MS(*m/z* 44 and 18, respectively). The contents of the released gases proved that the decomposition had taken place owing to the breakdown of the C–C and C–O bonds in the monosaccharide ring (Lakra et al. 2020). The DSC profile was in harmony

with the decomposition curve for the levan of *B. megaterium* PFY-147 (Pei et al. 2020). The EPS stopped to decompose at 596 °C, and its residual weight was 33.9%. Analysis of the differential thermogravimetric curve (DTG) showed that the EPS decomposition rate was highest at about 210 °C¾a temperature much lower than the degradation temperatures for the EPSs of *Bacillus tequilensis* FR9 (Rani et al. 2017) and *B. tequilensis* GM (Abid et al. 2019) (240 and 222 °C, respectively).

Topography and morphology of the EPS surface

SEM showed that the EPS was arranged in ragged sheets with smooth edges that ended with droplike structures of about 2 μm in diameter. The sheet surface was strewn with ovate-orbicular structures of about 4-5 μm in length and 1-2 μm in diameter (Fig. 4). Even under ×10,000 magnification, no appreciable deformations were observed on the sheet surface. Sheet morphology is characteristic of linear polysaccharides bound by multiple interchain H bonds. On the other hand, rounded and spherical structures are more typical of helical polysaccharides. Thus, the structure of the *C. salexigens* 3EQS1 EPS includes mostly H-bonded linear chains and some helical chains. The overall morphology of the EPS is in harmony with the previous report on the smooth-block surface of the levans produced by *Bacillus megaterium* PFY-147 (Pei et al. 2020).

The surface topography characteristics of the purified EPS were confirmed by AFM (Fig. 5). The surface was relatively smooth and had pits and pimples with a maximum amplitude of about 28 nm. Other researchers have reported thorny and spheroidal aggregates with a maximum height of 0.26 nm and with sizes of 95.3 to 300.13 nm, respectively (Pei et al. 2020; Iftikhar et al. 2021; Taylan et al. 2019).

Structural characterization of EPS

The size-exclusion chromatography elution profile showed that the EPS was a high-molecular-mass glycopolymer (Fig. S2). Fig. S3 shows the calibration curve of the serial dextran standards, which was plotted as the logarithmic molecular mass (lg Da) versus the retention time (R_t). Because dextrans elute with broadened peaks, we used the molecular masses of the peak maxima (M_p). On the basis of the calibration curve, the average molecular mass of the EPS was found to be 0.9×10^6 Da. Additional purification of the EPS by ion-exchange chromatography showed that the EPS lacked a negative charge. The EPS contained no contaminant proteins, and its carbohydrate content was about 99%. The monomer composition of the EPS was analyzed by HPAEC–PAD after acid hydrolysis. Only one peak was present, with the retention time corresponding to the standard of fructose (data not shown). This indicates that the EPS consisted solely of fructose residues.

The functional groups and the cycle size of the carbohydrate units were ascertained by FTIR spectroscopy. The FTIR spectrum of the EPS contained a broad intense band at 3446 cm^{-1}, assigned to the stretching vibrations of the H-bonded hydroxyl groups of the monosaccharide units and residual water (Fig. 6). The bands at 2954 and 2925 cm^{-1} were due to the antisymmetric stretching vibrations of the CH fragments, whereas the shoulders at around 2890 and 2854 cm^{-1} were due to the symmetric

stretching vibrations of the alkyl moieties. The broadened band at 1639 cm^{-1} was assigned to the bending mode of the hydroxyl groups, including those from water traces (Hashimoto and Kameoka 2000), and the weak shoulder at 1738 cm^{-1} was the C=O mode because of the small amounts of carboxyl groups. The absorption peaks at 1262 and 1412 cm^{-1} were due to C–H stretching and bending, respectively. These findings are in harmony with the data of the chemical composition analysis, which detected a single monomer¾fructose. The bands in the range 1150–1000 cm^{-1} were assigned to carbohydrate ring vibrations and C-OH/C-O-C modes. The low-frequency region contained overlapping bands at 927 and 808 cm^{-1}, characteristic of the furan ring. Thus, the FTIR spectrum confirmed that the EPS was a fructose polymer.

The ^{13}C NMR spectrum of the EPS (Fig. 7a) showed signals of a ketofuranose residue, including signals of one anomeric carbon atom, C(2), at δ 105.3 and signals of two hydroxymethyl groups, C(1) and C(6), at δ 61.2—64.5. The ^{1}H NMR spectrum (Fig. 7b) showed signals of six sugar protons at δ 3.57–4.18. The ^{1}H and ^{13}C NMR spectra were assigned by 2D NMR spectroscopy, including ^{1}H-^{1}H COSY, ^{1}H-^{13}C HSQC (Fig. S3), and ^{1}H-^{13}C HMBC experiments (Table 2). By comparing the ^{13}C chemical shifts with the published data (Bock and Pedersen 1983), the ketofuranose was identified as a β-fructofuranose. The linkage and sequence patterns were inferred from the ^{1}H-^{13}C HMBC spectrum, which showed C(2)/H(6b) interresidue correlations at 105.3/3.60 and 105.3/3.90. Therefore, the EPS is a linear fructan (levan) composed of →6)-β-d-Fru*f*-(2→ residues. The chemical shifts of the EPS were similar to those reported for levan (Barrow et al. 1984).

Table 2 ^{1}H and ^{13}C NMR data of the EPS from *C. salexigens* 3EQS1

Residue	H-1(a; b) C-1	H-2 C-2	H-3 C-3	H-4 C-4	H-5 C-5	H-6 (a; b) C-6
→6)-β-d-Fru*f*-(2→	3.67; 3.76 61.2	105.3	4.18 77.6	4.09 76.4	3.94 81.4	3.57; 3.89 64.5

Surfactant and emulsifying activities

Bacterial EPSs may have surfactant and emulsifying activities, increasing the availability of hydrophobic substrates to bacterial enzyme systems. In this study, the addition of a levan solution to the oil surface gave rise to a large and stable clear zone (64%). This indicates that the levan's biosurfactant properties were similar to those of the commercial surfactant in the oil displacement test.

Aqueous EPS solutions were examined for their ability to decrease the surface tension force arising at the air-liquid interface. This ability enables EPSs to act as surfactants and may be used in many technological processes. Measurements showed that in contrast to pure water, the levan solutions largely decreased the surface tension force (71.2 mN m^{-1} at 30 °C). Specifically, a 0.1% levan solution yielded a value of 62.7 ± 1.7 mN m^{-1} and the more concentrated 0.5% solution yielded an even lower value¾62.1 ±

1.9 mN m^{-1}. Thus, the levan reduced the surface tension by 11.9 and 12.7% (0.1 and 0.5% aqueous solution, respectively). Possibly, these close values are due to the same size of the aggregates formed by the solutions.

Because *C. salexigens* 3EQS1 produced large amounts of EPS, we analyzed the emulsifying activity of the EPS. This was found to be E_{24} 31.2 ± 0.4, 76.9 ± 1.3, and 98.9 ± 0.8% (E_{48} 31.2 ± 0.4, 68.6 ± 0.5, and 97.6 ± 0.6%) against kerosene, sunflower oil, and crude oil, respectively. Finally, the emulsions obtained with crude oil were stable after at least a few months.

An important variable in the characterization of the emulsifying and surfactant activities of polysaccharides is the CAC¾the concentration at which polymer aggregates are formed. DLS measurements yielded the levan concentration at which the light scattering intensity increased dramatically¾the CAC (about 240 µg mL^{-1}; Fig. S4). In aqueous solutions of both 0.5 and 1.0 mg mL^{-1} of the levan, nanosized supramolecular particles were found with certainty by DLS. The average hydrodynamic diameter (d) of these particles was 76 ± 4 nm. The most probable modal hydrodynamic diameter (d_m) was 68 ± 2 nm (Fig. S4). Thus, the levan formed aggregates at fairly low concentrations.

Discussion

The demand for natural ingredients in food, pharmaceuticals, and cosmetics is constantly growing. Owing to their wide range of properties, biodegradable and nontoxic microbial polysaccharides have potential for use in various biotechnologies (Giavasis 2013). These polymers include levan, a polyfructan produced by various bacteria and plants and used widely in industry as a sweetener, an emulsifier, a stabilizer, a thickener, an encapsulating agent, and a raw material for the production of “green” plastics (Wu et al. 2013). Bacterial levans are a product of the enzymatic conversion of sucrose. The main task in the production of levans is to maximize their yields and reduce the costs; this can be attained by optimization of bacterial growth conditions.

Halophiles can produce and accumulate fructans (Versluys et al. 2018). Bacterial growth under optimal conditions is not always attended by maximum EPS production. The EPS yield often depends on the nature and content of the carbon source (Lee et al. 1997). Husseiny et al. (2015) showed the ability of *C. salexigens* to produce levan and obtained the highest yield (11.9 g L^{-1}) when bacteria were grown at 30°C for 72 h and then left at 4°C for 48 h. In this study, *C. salexigens* 3EQS1 produced larger amounts of the levan (15.1 g L^{-1}) at 25°C for 72 h. In both Husseiny et al.’s and our studies, levan production was maximal at an NaCl concentration of 10–15% and an initial pH of 8conditions that reduced the possibility of bacterial culture contamination. The levan of *C. salexigens* 3EQS1 was found to be protein-free. Therefore, strain 3EQS1 has potential as a natural, safe, and highly effective levan producer.

Natural polysaccharides, including levans, are often heterogeneous in their molecular mass, which is caused by their different degrees of polymerization during biosynthesis. The molecular masses of bacterial levans are higher (> 500 kDa) than those of plant levans (Toksoy Öner et al. 2016). HPGPC showed that the levan of strain 3EQS1 has an average molecular mass of 0.9 MDa, which is typical of

bacterial levans. As is well known, many polysaccharides in aqueous solution form aggregates, and the levan of strain 3EQS1 likewise tends to form aggregates at fairly low concentrations, as shown by DLS. On the other hand, the bacterial synthesis of EPS is a labile process. The surface topography of synthesized EPSs in the solid state depends not only on their origin and chemical composition but also on their molecular mass. The surface of a dry levan sample may contain differently sized supramolecular particles. The sizes of the levan aggregates visualized by microscopy are expectedly smaller than those observed by DLS in solution owing to the presence of a solvate shell of water. SEM and AFM analysis of the surface morphology and the microstructural properties of the 3EQS1 levan can help to correlate the physicochemical properties of levans and levan-based materials. The revealed predominance of a compact sheet morphology indicates that the 3EQS1 levan is suitable for use in the production of plasticized films (Combie and Öner 2018) and, therefore, can be applied in the food industry or in nanotechnology.

Microbial molecules with high surface and emulsifying activities are classified as biosurfactants. These molecules reduce surface and interfacial tension both in aqueous solutions and in mixtures of hydrocarbons, making them potential agents for use in various biotechnologies and bioremediation (Bento et al. 2005). The 3EQS1 levan reduced the surface tension of water by about 12%, which is less than what can be achieved with other bacterial surfactants. This result is due to the absence of charged groups in levan structure and by the low degree of branching. Yet, the emulsifying/emulsion-stabilizing activity of the levan was high. After 24 h, the emulsion index (E_{24}) was highest with sunflower and crude oil (in the latter case, it was greater than 95%). The emulsions were stable for a long time. Thus, strain 3EQS1 offers promise for use in bioemulsifier production.

Conclusions

The results of this study establish that *C. salexigens* strain 3EQS1, isolated from a salt sample from Lake Qarun (Fayoum Province, Egypt), produces a high-molecular-mass (0.9 MDa) polyfructan. Precipitation from the culture medium with ethanol and fragmentation by gel filtration and anion-exchange chromatography yields a highly purified polysaccharide. Chemical analysis, FTIR spectroscopy, and NMR spectroscopy show that the β-d-(2→6)-linked fructan (levan) has a linear structure. Levan production is maximal (15 g L^{-1}) by 72 h of culture growth at 25 °C in a liquid mineral medium (initial pH 8.0) containing 10% sucrose and 10% NaCl. The substantial emulsifying and emulsion-stabilizing activities of the levan enable it to be used in various biotechnologies, including the food, cosmetic, and pharmaceutical industries, and in the bioremediation of soils polluted by petroleum hydrocarbons.

Declarations

Acknowledgments We acknowledge staff at the Simbioz Center for the Collective Use of Research Equipment in the Field of Physical–Chemical Biology and Nanobiotechnology (IBPPM RAS) for their technical support and provision of the FTIR and DLS equipment. We also thank Daniil Bratashov

(Remotely Controlled Theranostic Systems Lab, Scientific Medical Center, Saratov State University) for his help with SEM and AFM image acquisition.

Author contributions All authors contributed to the study conception and design. Material preparation, data collection and analysis were performed by Ibrahim M. Ibrahim, Elena N. Sigida, Vyacheslav S. Grinev, Maxim S. Kokoulin, Ivan G. Mokrushin, Gennady L. Burygin, Andrey M. Zakharevich, Alexander A. Shirokov, and Svetlana A. Konnova. The first draft of the manuscript was written by Yuliya P. Fedonenko, and all authors commented on previous versions of the manuscript. All authors read and approved the final manuscript.

Competing interest The authors have no relevant financial or non-financial interests to disclose.

References

1. Abid Y, Azabou S, Joulak I, Casillo A, Lanzetta R, Corsaro MM, Gharsallaoui A, Attia H (2019) Potential biotechnological properties of an exopolysaccharide produced by newly isolated *Bacillus tequilensis*-GM from spontaneously fermented goat milk. LWT 105:135–141. https://doi.org/10.1016/j.lwt.2019.02.005
2. Arahal DR, García MT, Vargas C, Cánovas D, Nieto JJ, Ventosa A (2001) *Chromohalobacter salexigens* sp. nov., a moderately halophilic species that includes *Halomonas elongata* DSM 3043 and ATCC 33174. Int J Syst Evol Microbiol 51:1457–1462. https://doi.org/10.1099/00207713-51-4-1457
3. Arahal DR, Vreeland RH, Litchfield CD, Mormile MR, Tindall BJ, Oren A, Bejar V, Quesada E, Ventosa A (2007) Recommended minimal standards for describing new taxa of the family *Halomonadaceae*. Int J Sys Evol Microbiol 57:2436–2446. https://doi.org/10.1099/ijs.0.65430-0
4. Argandoña M, Vargas C, Reina-Bueno M, Rodríguez-Moya J, Salvador M, Nieto JJ (2012) An extended suite of genetic tools for use in bacteria of the *Halomonadaceae*: an overview. In: Lorence A (ed) Recombinant gene expression, methods in molecular biology (methods and protocols), vol 824. Humana Press, Totowa NJ, pp 167–201. https://doi.org/10.1007/978-1-61779-433-9_9
5. Aurell CA, Wistrom AO (1998) Critical aggregation concentrations of gram-negative bacterial lipopolysaccharides (LPS). Biochem Biophys Res Commun 253:119–123. https://doi.org/10.1006/bbrc.1998.9773
6. Barrow KD, Collins JG, Rogers PL, Smith GM (1984) The structure of a novel polysaccharide isolated from *Zymomonas mobilis* determined by nuclear magnetic resonance spectroscopy. Eur J Biochem 145:173–179. https://doi.org/10.1111/j.1432-1033.1984.tb08537.x
7. Bento FM, de Oliveira Camargo FA, Okeke BC, Frankenberger WT (2005) Diversity of biosurfactant producing microorganisms isolated from soils contaminated with diesel oil. Microbiol Res 160(3):249–255. https://doi.org/10.1016/j.micres.2004.08.005
8. Bock K, Pedersen C (1983) Carbon-13 nuclear magnetic resonance spectroscopy of monosaccharides. Adv Carbohydr Chem Biochem 41:27–66. https://doi.org/10.1016/S0065-

2318(08)60055-4

9. Bradford MM (1976) A rapid and sensitive method for the quantitation of microgram quantities of protein utilizing the principle of protein-dye binding. Anal Biochem 72:248–254. https://doi.org/10.1016/0003-2697(76)90527-3
10. Burygin GL, Sigida EN, Fedonenko YP, Khlebtsov BN, Shchyogolev SY (2016) The use and development of the dynamic light-scattering method to investigate supramolecular structures in aqueous solutions of bacterial lipopolysaccharides. Biophysics 61:547–557. https://doi.org/10.1134/S0006350916040059
11. Chen GQ, Jiang XR (2018) Next generation industrial biotechnology based on extremophilic bacteria. Curr Opin Biotechnol 50:94–100. https://doi.org/10.1016/j.copbio.2017.11.016
12. Cooper DG, Goldenberg BG (1987) Surface-active agents from two *Bacilllus* species. Appl Environ Microbiol 53:224–229
13. Corral P, Amoozegar MA, Ventosa A (2020) Halophiles and their biomolecules: recent advances and future applications in biomedicine. Mar Drugs 18:33. https://doi.org/10.3390/md18010033
14. Combie J, Öner ET (2018) From healing wounds to resorbable electronics, levan can fill bioadhesive roles in scores of markets. Bioinspir Biomim 14(1):011001. https://doi.org/10.1088/1748-3190/aaed92
15. de la Haba RR, Sánchez-Porro C, Ventosa A (2011) Taxonomy, phylogeny, and biotechnological interest of the family *Halomonadaceae*. In: Ventosa A, Oren A, Ma Y (eds) Halophiles and hypersaline environments. Springer, Springer, Berlin, Heidelberg, pp 27–64. https://doi.org/10.1007/978-3-642-20198-1_3
16. Djurić A, Gojgić-Cvijović G, Jakovljević D, Kekez B, Stefanović Kojić J, Mattinen M-L, Harju IE, Vrvić MM, Beškoski VP (2017) *Brachybacterium* sp. CH-KOV3 isolated from an oil-polluted environment – a new producer of levan. Int J Biol Macromol 104:311–321. https://doi.org/10.1016/j.ijbiomac.2017.06.034
17. DuBois M, Gilles KA, Hamilton JK, Rebers PA, Smith F (1956) Colorimetric method for determination of sugars and related substances. Anal Chem 28:350–356. https://doi.org/10.1021/ac60111a017
18. Edbeib MF, Wahab RA, Huyop F (2016) Halophiles: biology, adaptation, and their role in decontamination of hypersaline environments. World J Microbiol Biotechnol 32:135. https://doi.org/10.1007/s11274-016-2081-9
19. Fathepure BZ (2014) Recent studies in microbial degradation of petroleum hydrocarbons in hypersaline environments. Front Microbiol 5:173. https://doi.org/10.3389/fmicb.2014.00173
20. Giavasis I (2013) 16 - Production of microbial polysaccharides for use in food. In: McNeil B, Archer D, Giavasis I, Harvey L (eds) Technology and nutrition, microbial production of food ingredients, enzymes and nutraceuticals. Woodhead publishing series in food science. Woodhead Publishing, pp 413–468. https://doi.org/10.1533/9780857093547.2.413
21. Hashimoto A, Kameoka T (2000) Mid-infrared spectroscopic determination of sugar contents in plant-cell culture media using an ATR method. Appl Spectrosc 54:1005–1011.

https://doi.org/10.1366/0003702001950490

22. Husseiny SM, Sheref FA, Amer H, Elsakhawy TA (2015) Biosynthesis of applicable levan by a new levan producing moderately halophilic strain *Chromohalobacter salexigens* and its biological activities. Curr Sci Int 4:423–434
23. Huval JH, Latta R, Wallace R, Kushner DJ, Vreeland RH (1995) Description of two new species of *Halomonas*: *Halomonas israelensis* sp. nov. and *Halomonas canadensis* sp. nov. Can J Microbiol 41:1124–1131. https://doi.org/10.1139/m95-156
24. Ibrahim IM, Konnova SA, Sigida EN, Lyubun EV, Muratova AYu, Fedonenko YuP, Elbanna K (2020) Bioremediation potential of a halophilic *Halobacillus* sp. strain, EG1HP4QL: exopolysaccharide production, crude oil degradation, and heavy metal tolerance. Extremophiles 24:157–166. https://doi.org/10.1007/s00792-019-01143-2
25. Iftikhar R, Ansari A, Siddiqui NN, Hussain F, Aman A (2021) Structural elucidation and cytotoxic analysis of a fructan based biopolymer produced extracellularly by *Zymomonas mobilis* KIBGE-IB14. Carbohydr Res 499:108223. https://doi.org/10.1016/j.carres.2020.108223
26. Kazak Sarilmişer H, Ates O, Ozdemir G, Arga KY, Toksoy Öner E (2015) Effective stimulating factors for microbial levan production by *Halomonas smyrnensis* AAD6T. J Biosci Bioeng 119(4):455–463. https://doi.org/10.1016/j.jbiosc.2014.09.019
27. Kekez BD, Gojgic-Cvijovic GD, Jakovljevic DM, Stefanovic Kojic JR, Markovic MD, Beskoski VP, Vrvic MM (2015) High levan production by *Bacillus licheniformis* NS032 using ammonium chloride as the sole nitrogen source. Appl Biochem Biotechnol 175:3068–3083. https://doi.org/10.1007/s12010-015-1475-8
28. Khalil CA, Prince VL, Prince RC, Greer CW, Lee K, Zhang B, Boufadel MC (2021) Occurrence and biodegradation of hydrocarbons at high salinities. Sci Total Environ 762:143165. https://doi.org/10.1016/j.scitotenv.2020.143165
29. Kim OS, Cho YJ, Lee K, Yoon SH, Kim M, Na H, Park SC, Jeon YS, Lee JH, Yi H, Won S, Chun J (2012) Introducing EzTaxon-e: a prokaryotic 16S rRNA gene sequence database with phylotypes that represent uncultured species. Int J Syst Evol Microbiol 62:716–721. https://doi.org/10.1099/ijs.0.038075-0
30. Kirtel O, Versluys M, den Ende WV, Toksoy Öner E (2018) Fructans of the saline world. Biotechnol Adv 36:1524–1539. https//doi.org/10.1016/j.biotechadv.2018.06.009
31. Lakra AK, Domdi L, Tilwani YM, Arul V (2020) Physicochemical and functional characterization of mannan exopolysaccharide from *Weissella confusa* MD1 with bioactivities. Int J Biol Macromol 143:797–805. https://doi.org/10.1016/j.ijbiomac.2019.09.139
32. Ławniczak Ł, Woźniak-Karczewska M, Loibner AP, Heipieper HJ, Chrzanowski Ł (2020) Microbial degradation of hydrocarbons—basic principles for bioremediation: a review. Molecules 25(4):856. https://doi.org/10.3390/molecules25040856
33. Le Borgne S, Paniagua D, Vazquez-Duhalt R (2008) Biodegradation of organic pollutants by halophilic bacteria and archaea. J Mol Microbiol Biotechnol 15:74–92.

https://doi.org/10.1159/000121323

34. Lee IY, Seo WT, Kim GJ, Kim MK, Ahn SG, Kwon GS, Park YH (1997) Optimization of fermentation conditions for production of exopolysaccharide by *Bacillus polymyxa*. Bioproc Engin 16:71–75. https://doi.org/10.1007/s004490050290
35. Lefort V, Desper R, Gascuel O (2015) FastME 2.0: a comprehensive, accurate, and fast distance-based phylogeny inference program. Mol Biol Evol 32:2798–2800. https://doi.org/10.1093/molbev/msv150
36. Mendonça CMN, Oliveira RC, Freire RKB, Piazentin ACM, Pereira WA, Gudiña EJ, Evtuguin DV, Converti A, Santos JHPM, Nunes C, Rodrigues LR, Oliveira RPS (2021) Characterization of levan produced by a *Paenibacillus* sp. isolated from Brazilian crude oil. Int J Biol Macromol 186:788–799. https://doi.org/10.1007/s12010-015-1475-8
37. Nečas D, Klapetek P, Ondrasek G, Rengel Z (2012) (2021) Environmental salinization processes: Detection, implications and solutions. Sci Total Environ 754:142432 https//doi.org/10.1016/j.scitotenv.2020.142432
38. Oren A (2010) Industrial and environmental applications of halophilic microorganisms. Environ Technol 31:825–834. https//doi.org/10.1080/09593330903370026
39. Oren A (2015) Halophilic microbial communities and their environments. Curr Opin Biotechnol 33:119–124. https://doi.org/10.1016/j.copbio.2015.02.005
40. Pei F, Ma Y, Chen X, Liu H (2020) Purification and structural characterization and antioxidant activity of levan from *Bacillus megaterium* PFY-147. Int J Biol Macromol 161:1181–1188. https://doi.org/10.1016/j.ijbiomac.2020.06.140
41. Rani RP, Anandharaj M, Sabhapathy P, Ravindran AD (2017) Physiochemical and biological characterization of novel exopolysaccharide produced by *Bacillus tequilensis* FR9 isolated from chicken. Int J Biol Macromol 96:1–10. https://doi.org/10.1016/j.ijbiomac.2016.11.122
42. Rodrigues LR, Teixeira JA, van der Mei HC, Oliveira R (2006) Physicochemical and functional characterization of a biosurfactant produced by *Lactococcus lactis* 53. Colloids Surf B 49:79–86. https://doi.org/10.1016/j.colsurfb.2006.03.003
43. Sehgal SN, Gibbons NE (1960) Effect of some metal ions on the growth of *Halobacterium cutirubrum*. Can J Microbiol 6(2):165–169. https://doi.org/10.1139/m60-018
44. Sorokin DY, Janssen AJ, Muyzer G (2012) Biodegradation potential of halo(alkali)philic prokaryotes. Crit Rev Environ Sci Technol 42:811–856. https://doi.org/10.1080/10643389.2010.534037
45. Taylan O, Yilmaz MT, Dertli E (2019) Partial characterization of a levan type exopolysaccharide (EPS) produced by *Leuconostoc mesenteroides* showing immunostimulatory and antioxidant activities. Int J Biol Macromol 136:436–444. https://doi.org/10.1016/j.ijbiomac.2019.06.078
46. Toksoy Öner E, Hernández J, Combie J (2016) Review of levan polysaccharide: from a century of past experiences to future prospects. Biotechnol Adv 34:827–844. https://doi.org/10.1016/j.biotechadv.2016.05.002

47. Ventosa A, Nieto JJ, Oren A (1998) Biology of moderately halophilic aerobic bacteria. Microbiol Mol Biol Rev 62:504–544. https://doi.org/10.1128/MMBR.62.2.504-544.1998
48. Versluys M, Kirtel O, Toksoy Öner E, Van den Ende W (2018) The fructan syndrome: evolutionary aspects and common themes among plants and microbes. Plant Cell Environ 41(1):16–38. https://doi.org/10.1111/pce.13070
49. Wu D, Cai S, Chen M, Ye L, Chen L, Zhang H, Dai F, Wu F, Zhang G (2013) Tissue metabolic responses to salt stress in wild and cultivated barley. PLoS ONE 8(1):e55431. https://doi.org/10.1371/journal.pone.0055431
50. Zhuang X, Han Z, Bai Z, Zhuang G, Shim H (2010) Progress in decontamination by halophilic microorganisms in saline wastewater and soil. Environ Pollut 158(5):1119–1126. https://doi.org/10.1016/j.envpol.2010.01.007

Figures

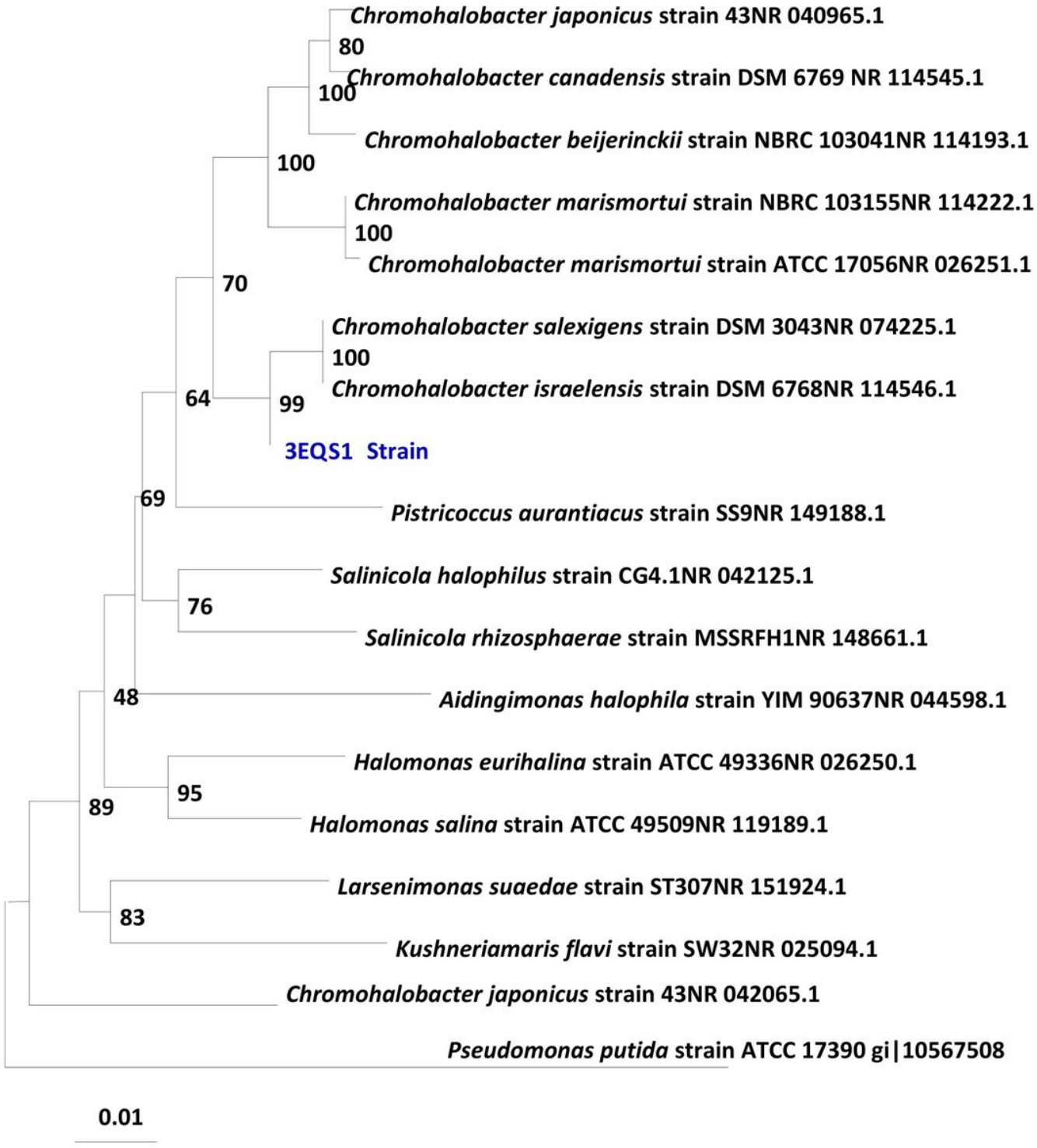

Figure 1

Phylogenetic neighbor-joining tree based on 16S rDNA sequence of strain 3EQS1. Bootstrap values (expressed as percentages of 1000 replications) are shown at branch nodes.

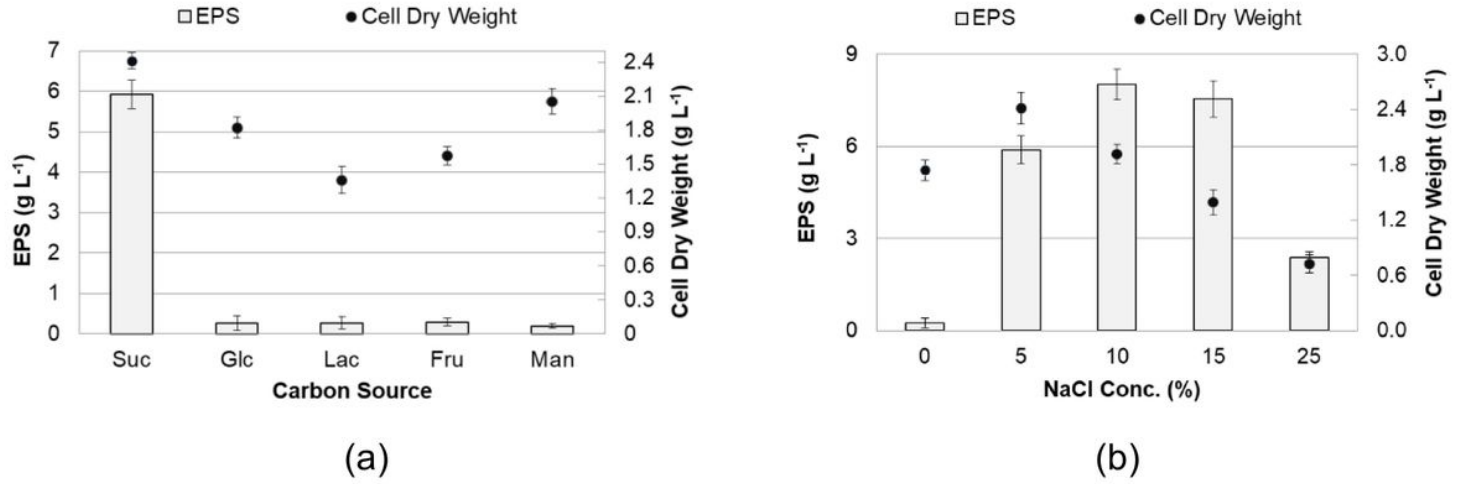

Figure 2

Effect of carbon source (a) and NaCl concentration (b) on growth and EPS production in strain 3EQS1. For growth conditions for each experiment, see Materials and methods

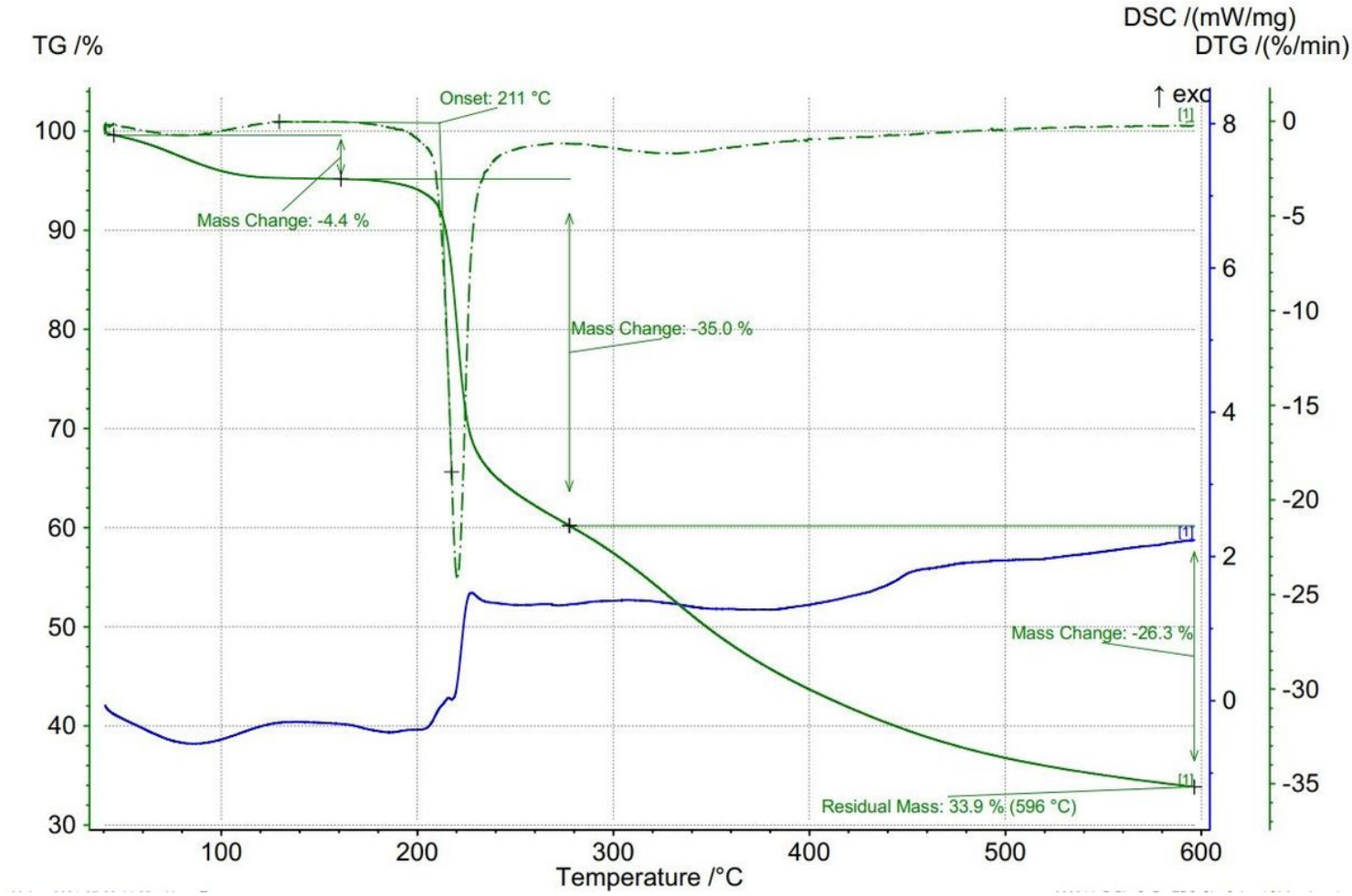

Figure 3

TGA-DSC-DTG diagram of the *C. salexigens* 3EQS1 EPS

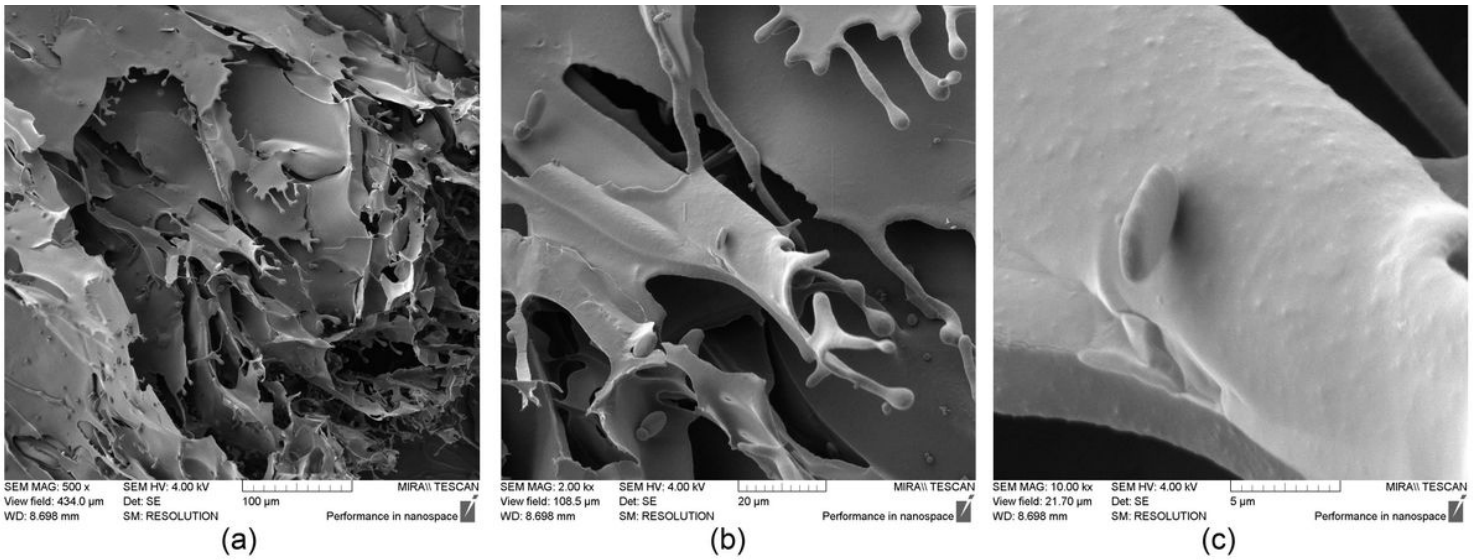

Figure 4

SEM of the *C. salexigens* 3EQS1 EPS. Magnification: 500´ (a), 2000× (b), 10,000´ (c)

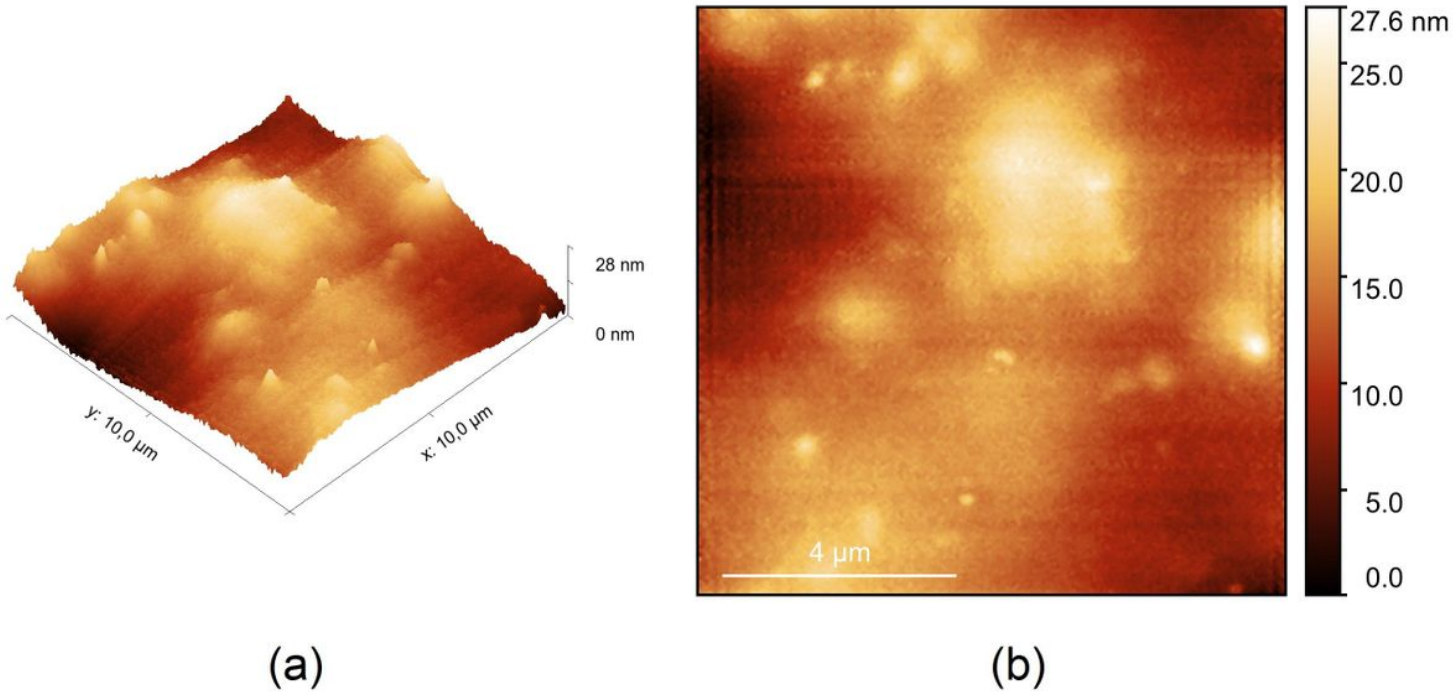

Figure 5

Surface topology of a sheet fragment for the *C. salexigens* 3EQS1 EPS (AFM): 3D image (a); 2D image (b)

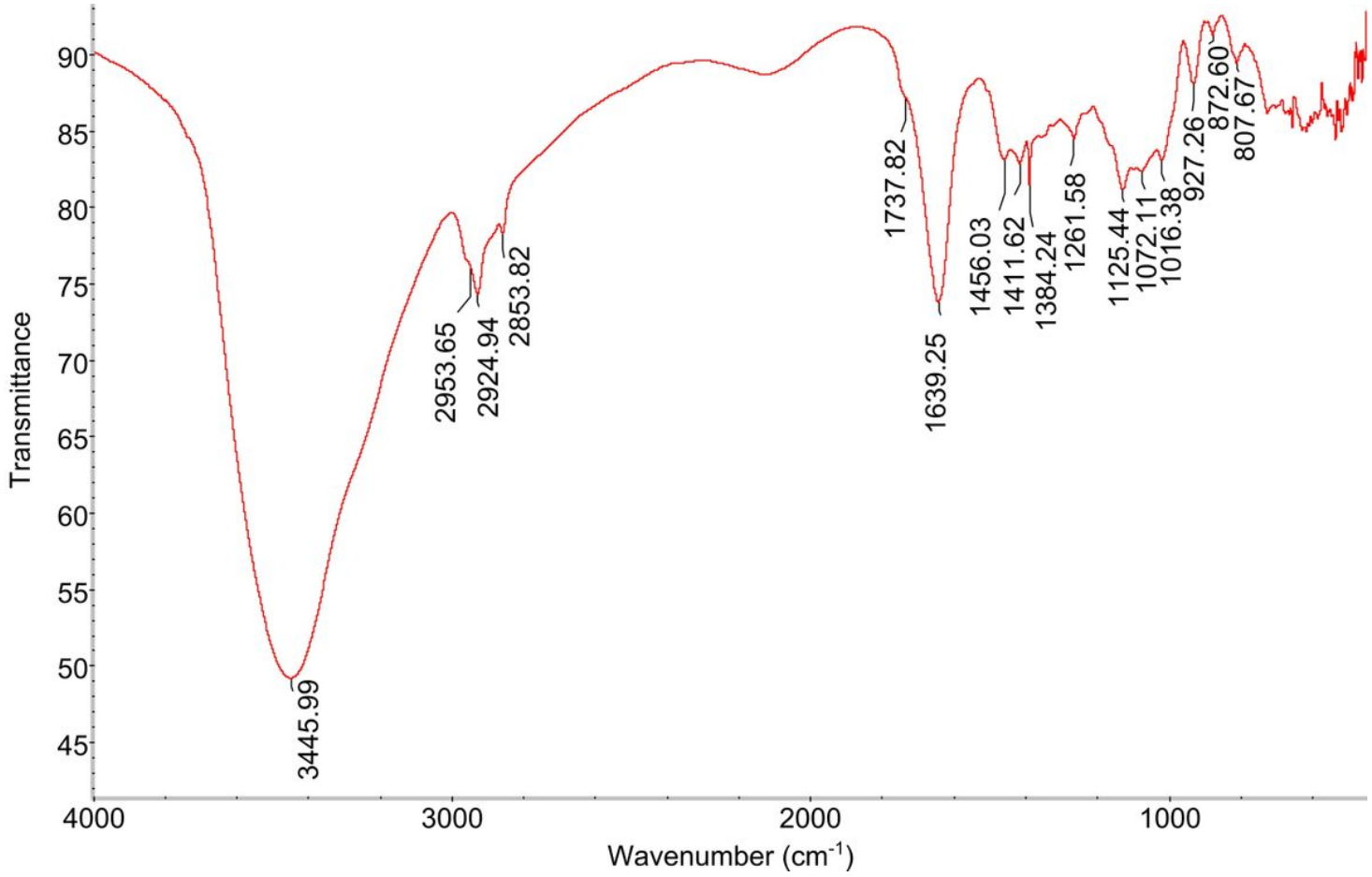

Figure 6

FTIR spectrum of the *C. salexigens 3EQS1* EPS

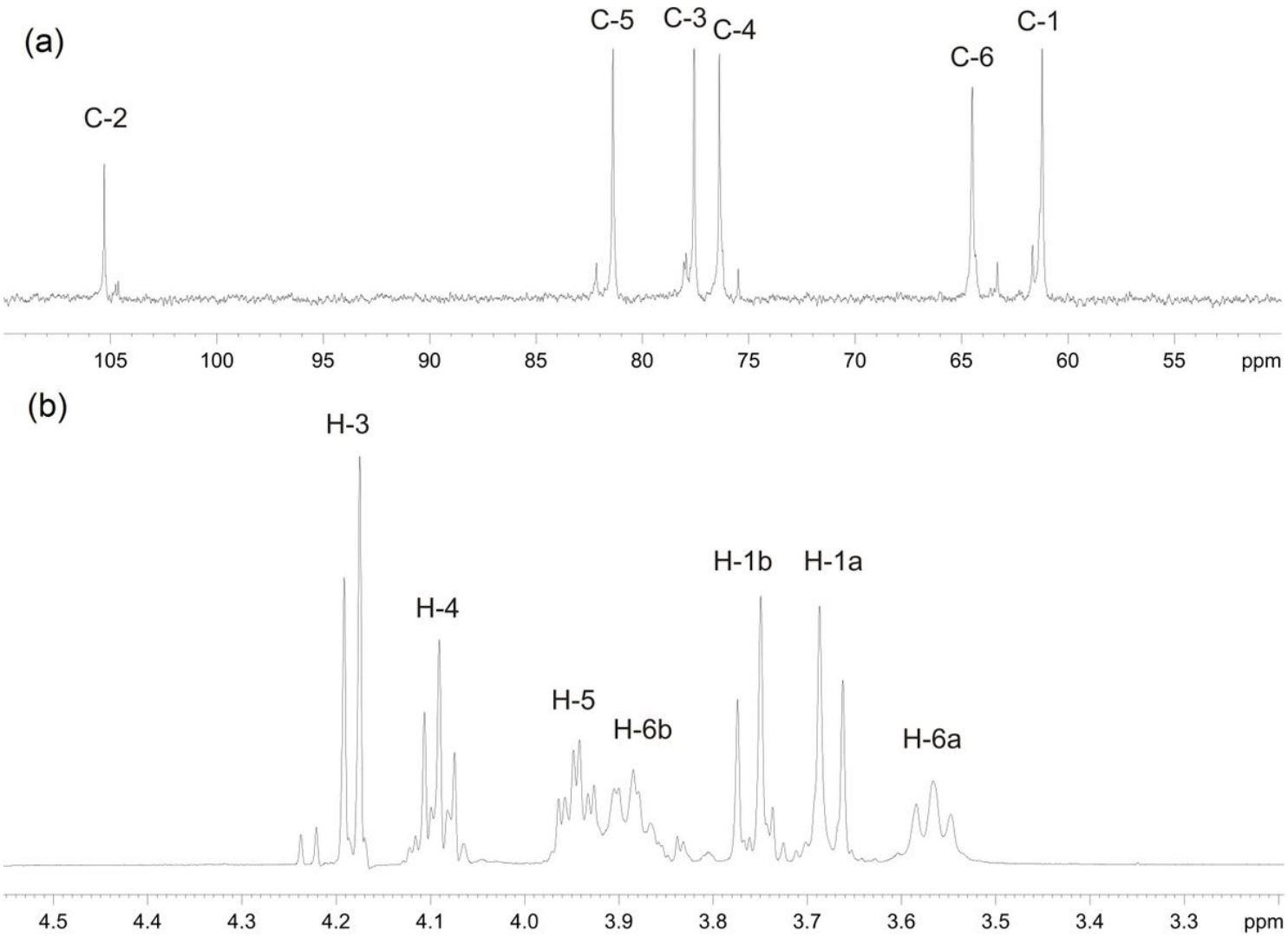

Figure 7

^{13}C (a) and ^{1}H (b) NMR spectra of the *C. salexigens* 3EQS1 EPS

Supplementary Files

This is a list of supplementary files associated with this preprint. Click to download.

- Supplemetaryinformation.docx